The 39^{th} International Workshop on Water Waves and Floating Bodies, 14-17 April 2024, St Andrews, Scotland

Numerical simulations of the breaking of short-crested waves in deep water

Ayoub Mansar[a], **Frederic Dias**[a ,b]

a. ENS Paris-Saclay, CNRS, Centre Borelli, Université Paris-Saclay, Gif-sur-Yvette 91190, France

b. School of Mathematics and Statistics, University College Dublin, Belfield, Dublin 4, Ireland

Email: ayoub.mansar@ens-paris-saclay.fr

Highlights

- A two-phase Navier-Stokes solver has been successfully applied to simulate the breaking of a family of short-crested waves in deep water.
- The effect of the obliquity, initial slope and surface tension on some commonly used breaking criterias and energy dissipation is determined for a range of parameters.

1 Introduction

The breaking of ocean waves contributes significantly to wave energy dissipation and marks the transition from laminar flow to turbulent mixing at smaller scales on the ocean surface. The implications of wave breaking extend to particle transport, influencing the fate of oil spills and plastic pollutants. To predict water surface changes, energy loss and turbulence accurately, numerical codes must incorporate breaking criteria and mathematical models for energy dissipation. Over the past seven decades, numerous breaking onset criteria have been proposed through theoretical studies, numerical simulations, laboratory experiments, and field observations, falling into three main categories: geometric, kinematic, and dynamic. A recent overview can be found in [1].

The recent development in computation capacity and numerical methods made DNS simulations of breaking waves feasible. Recent studies have focused on the complete resolution of the breaking of analytical Stokes solutions, either in 2D or 3D with different resolutions. For instance, Deike et al. [2] examined the effect of capillarity on the breaking regime and dissipation, while in [3] they focused on air entrainment and bubble statistics. Mostert et al. [4] conducted a parametric study on energy dissipation, considering the turbulent Reynolds number and the Bond number. Wu et al. [5] investigated the wind wave growth. These studies have shown the ability of DNS to resolve the mixing transition in turbulent multiphase flows with a reasonable agreement with available laboratory data [4].

In contrast to the examination of Stokes waves which exhibit regularity in terms of their wave crests, our study deviates by examining the breaking of the simplest non-trivial three-dimensional waves: The short-crested wave system, defined as doubly periodic waves in the plane. This wave system, more prevalent in nature than its two-dimensional counterparts on complex oceanic surfaces, is generated within a wind fetch, from intersecting swell waves, or leeward of offshore islands or structures due to diffracted wave interactions [6].

In this study, we conduct a parametrical study in terms of the independent parameters of the simulation, in order to study the effect of the wave obliquity and intial slope on

the breaking onset geometrical and kinematic criterias and on the corresponding energy dissipation of short-crested waves.

2 Mathematical model

We use Basilisk, a software package available as open-source, that enables the solution of diverse partial differential equation systems across various mesh types. More specifically, we utilize the two-phase flow Navier-Stokes solver with surface tension in three dimensions. The incompressible, variable density, Navier-Stokes equations with surface tension can be expressed as :

$$\begin{aligned}
&\frac{\partial \rho}{\partial t} + \nabla \cdot (\rho \mathbf{u}) = 0, \\
&\rho \left(\frac{\partial \mathbf{u}}{\partial t} + \mathbf{u} \cdot \nabla \mathbf{u} \right) = -\nabla p + \nabla \cdot (2\mu \mathbf{D}) + \rho \mathbf{g} + \sigma \kappa \delta_s \mathbf{n} \\
&\nabla \cdot \mathbf{u} = 0
\end{aligned}$$

where $\mathbf{u} = (u, v, w)$ is the fluid velocity, $\rho = \rho(\mathbf{x}, t)$ the fluid density, $\mu = \mu(\mathbf{x}, t)$ the dynamic viscosity, $\mathbf{D}$ is the deformation tensor defined as $D_{ij} = (\partial_i u_j + \partial_j u_i)/2$, σ the surface tension coefficient, κ the curvature of the interface, $\mathbf{n}$ its unit normal vector. The concentration of the surface tension term at the fluid interface is represented by the Dirac delta function δ_s.

The density and viscosity values depend on the local volume fraction in each cell according to a volume fraction field $\tau(\mathbf{x}, t)$ set to zero in the gas phase and one in the liquid phase.

3 Numerical simulations

The study is conducted in terms of non-dimensional parameters, considering the following relevant physical parameters: liquid and gas density (ρ_w, ρ_a), dynamic viscosities (μ_w, μ_a), surface tension (σ), Wavelengths in the $x-$ and $z-$ directions (λ_x,λ_z), Initial wave amplitude (a_0), acceleration due to gravity (g), Water depth (h_0). These parameters can be expressed in terms of dimensionless quantities : density ratio (ρ_a/ρ_w), viscosity ratio (μ_a/μ_w), initial wave slope ($S = a_0 k$), Bond number ($Bo = \Delta\rho g/\sigma k^2$), Reynolds number ($Re = \sqrt{g\lambda^3}/\nu_w$) and the incident/reflected wavelengths ratio ($\lambda_y/\lambda_x = \sin(\theta)/\cos(\theta) = \tan(\theta)$).

The numerical domain used in this study is a cuboid with dimensions corresponding to the wavelengths in the $x-$ and $z-$ directions, The length of the cuboid in the $x-$direction, denoted as L_x, is equal to the wavelength in the $x-$direction $L_x = \lambda_x = \lambda/\sin(\theta)$, where λ is chosen equal to 1. Similarly, the lengths of the cuboid in the $y-$ and $z-$ directions, denoted as L_y and L_z respectively, are equal to the wavelength in the $z-$direction λ_z calculated as $L_y = L_z = \lambda/\cos(\theta)$.

The wave is set to travel in the $x-$direction within the numerical domain. Periodic boundary conditions are applied in both the $x-$ and $z-$ directions, allowing the wave pattern to repeat periodically along these axes, and free-slip boundary conditions are specified at the top and bottom of the domain.

4 Results and Discussion

We systematically vary several parameters in our simulations, including the initial slope (S) in the range of $[0.3-0.8]$ and the Bond number (BO) in the range of $[200-1000]$, for specific θ values ($26°$, $45°$, $63°$). These three angles allow a discrete transition between two short-crested wave limits: the 2D progressive wave obtained for $\theta = 90°$ and the standing wave limit obtained for $\theta = 0°$. In Figure 1, we illustrate an example of the breaking of a plunging Short-Crested Wave (SCW) in the gravity wave regime with negligible surface tension ($BO = 1000$).

The initially unstable wave propagates and steepens, and breaking onset occurs at approximately $t = 0.3T_0$, where T_0 is the linear time period. At $t = 0.6T_0$, a jet forms at the top center of the region connecting the crests of the short-crested wave system. By $t = 0.9T_0$, the jet reconnects with the wave, resulting in both splash-up and the formation of bubbles due to air cavity entrainment by the jet.

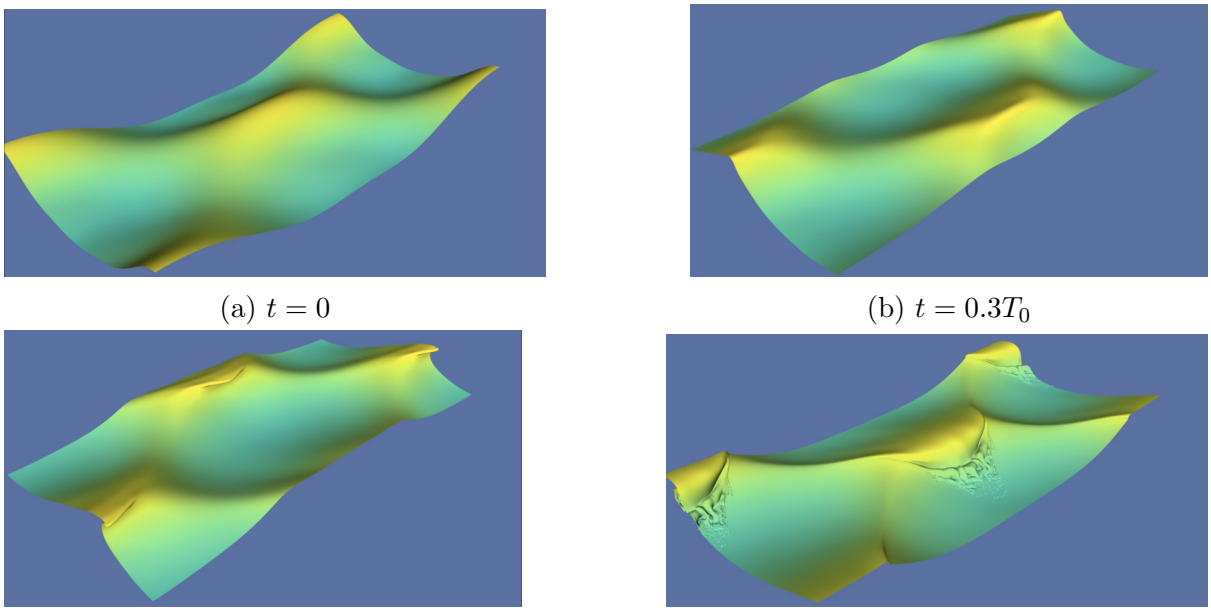

(a) $t = 0$ (b) $t = 0.3T_0$

(c) $t = 0.6T_0$ (d) $t = 0.9T_0$

Figure 1: Breaking of short-crested wave initialized with parameters $BO = 1000$, $\theta = 63.43°$ and $S = 0.65$

To characterize wave breaking for this family of 3D waves, we examine common geometrical (local steepness, local slope, local curvature) and kinematic (particle speed to crest speed ratio u/c) parameters. For instance, in Figure 2, we present the measured Gaussian curvature (κ) as a spilling breaking SCW with moderate surface tension effects $BO = 200$, initialized with parameters ($\theta = 45°$, $S = 0.65$), propagates. The evolving Gaussian curvature values on the free surface reveal a growing breaking crest region, defining a contour of the breaking crest.

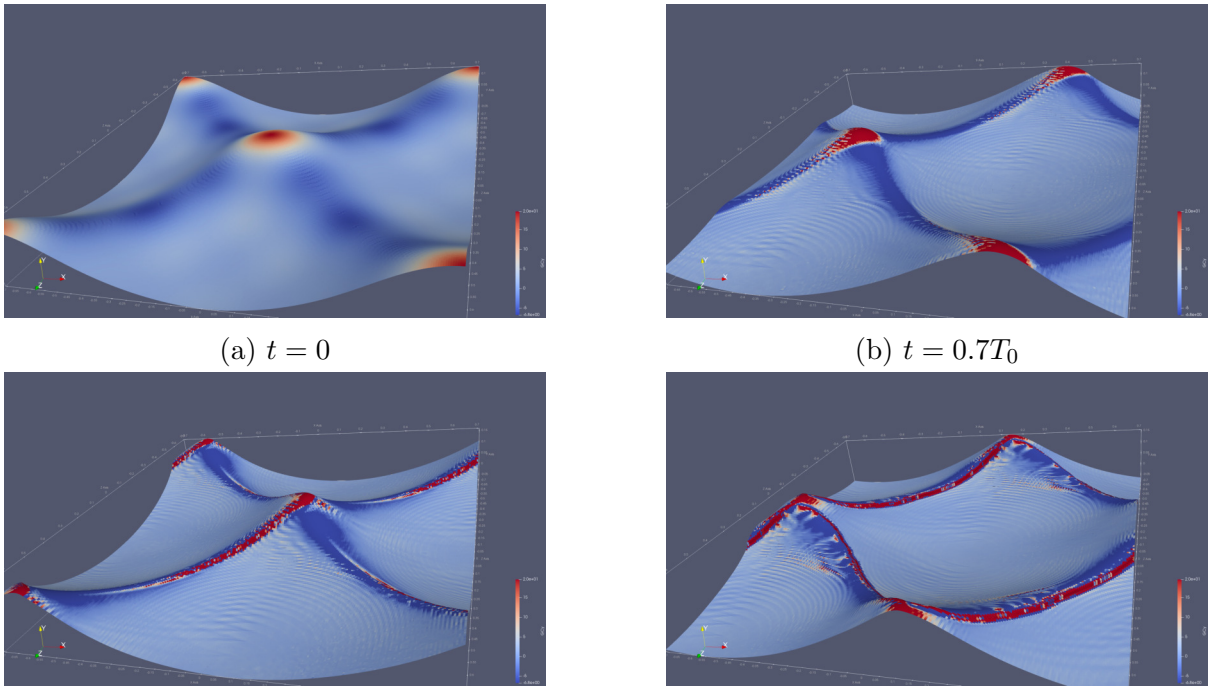

(a) $t = 0$ (b) $t = 0.7T_0$

(c) $t = T_0$ (d) $t = 1.5T_0$

Figure 2: Evolution of the Gaussian curvature computed at the free surface for a short-crested wave with initial parameters ($\theta = 45°$, $BO = 200$, $S = 0.65$)

We propose to examine the length of the breaking crest by evaluating the geometrical and kinematic breaking onset criteria measured on the free surface across a range of parameters. The outcomes of this analysis, along with insights into energy dissipation, will be presented during the workshop.

References

[1] Marc Perlin, Wooyoung Choi, and Zhigang Tian. Breaking waves in deep and intermediate waters. *Annual Review of Fluid Mechanics*, 45:115–145, 01 2013.

[2] Luc Deike, Stephane Popinet, and W. Kendall Melville. Capillary effects on wave breaking. *Journal of Fluid Mechanics*, 769:541–569, 2015.

[3] Luc Deike, W. Kendall Melville, and Stéphane Popinet. Air entrainment and bubble statistics in breaking waves. *Journal of Fluid Mechanics*, 801:91–129, 2016.

[4] W. Mostert, S. Popinet, and L. Deike. High-resolution direct simulation of deep water breaking waves: transition to turbulence, bubbles and droplets production. *Journal of Fluid Mechanics*, 942:A27, 2022.

[5] Jiarong Wu, Stéphane Popinet, and Luc Deike. Revisiting wind wave growth with fully coupled direct numerical simulations. *Journal of Fluid Mechanics*, 951:A18, 2022.

[6] C.P. Tsai, D.S. Jeng, and J.R.C. Hsu. Computations of the almost highest short-crested waves in deep water. *Applied Ocean Research*, 16(6):317–326, 1994.